The Fourth IEEE RAS/EMBS International Conference
on Biomedical Robotics and Biomechatronics
Roma, Italy. June 24-27, 2012

Index Finger Rehabilitation/Assistive Device

Andrea Polotto, Francesco Modulo, Fabio Flumian, Zhen Gang Xiao, Paolo Boscariol, Carlo Menon

Abstract—**In this paper, a novel exoskeleton for the index finger is introduced. Such a device is intended to be used for the rehabilitation of post-stroke patients. The target of the design is to produce a device with low weight and reduced space occupation, so that it can be worn without interfering with everyday use of the hand. The actuation is provided using low-cost lightweight miniature DC motors, and position feedback is obtained trough potentiometers. A working prototype has been built and tested. A closed-loop position control with friction compensation has been implemented and experimental results are presented and discussed.**

I. Introduction

A stroke occurs when a blood vessel that carries oxygen and nutrients to the brain is either blocked by a clot or bursts. It often causes body impairments to the survivors, which seriously decrease the quality of life.

Physical rehabilitation is available to regain some lost function; however, it is very labour intensive and costly. The problem of the stroke is very widespread in the world. For example, according to the Heart and Stroke Foundation of Canada, there are over 50,000 strokes in Canada each year [1]. Several researchers have proposed the use of robotic devices as a way to improve the effectiveness of the rehabilitation process [2].

The hand is one of the most used and difficult parts of the body to be rehabilitated. Despite the challenge, devices like Myoelectric Hand Orthosis [3] have been presented in academic paper in early 90's. In general, the hand rehabilitation devices can be divided in two categories. One focuses on hand rehabilitation through simple movements, such as hand grasping or extension of the fingers with limited degree of control. Devices like Rutger master II [4], Gentle/g system [5] and a pneumatic muscle hand therapy device in [6] belong to this category. The other type of hand rehabilitation devices [7]-[11] is capable of providing control on each individual finger joint in order to perform more complex finger rehabilitation routines. Among these, devices presented in [9]-[11] could potentially be used as an assistive device during the activity of daily living, if their portability could be improved. Portability is a critical aspect to allow the use of these devices in domestic environments, such as the users' homes, and consequently increase the frequency and decrease the cost of rehabilitation.

The aim of this paper is to introduce a novel rehabilitation/assistive device for the index finger, which has a compact and light weight design, as well as full control of each finger's joint. Due to the peculiar structure of the human hand, this device can be used for the other fingers as well, with the exception of the thumb, which has a different kinematic configuration. The mechanical design of the exoskeleton is described in Section II. The design and performance of a position tracking controller with friction compensation are presented in Section III and the conclusion is presented in Section IV.

II. Mechanical Design

A. The Index Finger

The human hand consists of four fingers and one thumb. All the fingers have the same structure, which consists of three joints and three phalanxes. The design presented here is based on the index finger, but it can be easily adapted to the other three fingers as well. A simplified schematic of the index finger is shown in Fig 1. The three joints are the metacarpophalangeal (MCP) joint, the proximal interphalangeal (PIP) joint and the distal interphalangeal (DIP) joint. The MCP joint links the metacarpal bone and the proximal phalanx; it has two degrees of freedom (DOF) since it allows both the abduction/adduction and the flexion/extension motion. The PIP joint links the proximal and the medial phalanxes, while the DIP joint links the medial and the distal phalanxes; each of them has one DOF, which only allows flexion/extension. The flexion/extension range of motion for the index finger is greater at the PIP joint (from 100 to 110 deg) than it is at the DIP joint (typically around 80 deg). Moreover the DIP joint may have some passive hyperextension (around 15 deg), but the PIP joint has essentially none in most individuals [12].

B. Overview of the Mechanical System

The CAD drawing of the overall mechanical system is shown in Fig 2. The system can be separated into three independent modules: they are the MCP joint module, the PIP joint module and the DIP joint module. Micro-geared DC motors (Pololu HP series) have been selected for all the

Manuscript received January 30th, 2012. This work was supported by the Natural Sciences and Engineering Research Council of Canada (NSERC) and the Canadian Institutes of Health Research (CIHR).

A. Polotto, F. Modulo, F. Flumian, and Z.G. Xiao are with the MENRVA Group, School of Engineering Science, Simon Fraser University, Burnaby, BC V5A 1S6 Canada. (e-mail: andrea.polotto@gmail.com; valoreassoluto@hotmail.com; fabioflumian@gmail.com; zgx@sfu.ca).

P. Boscariol is with Dipartimento di Ingegneria Elettrica, Gestionale e Meccanica, Università degli Studi di Udine, Via delle Scienze 208, 33100 Udine, Italy (e-mail: paolo.boscariol@uniud.it)

C. Menon is an Assistant Professor with the MENRVA Group, School of Engineering Science, Simon Fraser University, Burnaby, BC V5A 1S6 Canada. (phone: 1-778-782-6860; fax: 1-778-782-4951; e-mail: cmenon@sfu.ca).

Contact author: C. Menon (e-mail: cmenon@sfu.ca).

actuation modules because of their high torque to weight ratio, which allows a compact and lightweight design. A detailed descriptions of the modules is presented in subsections C and D.

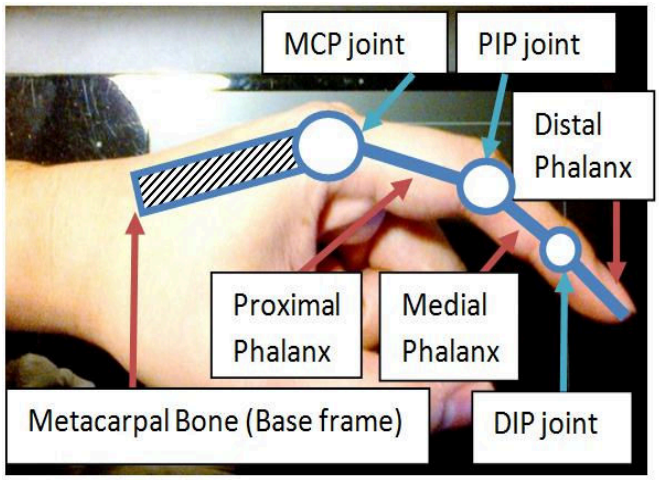

Fig. 1. Representation of the index finger.

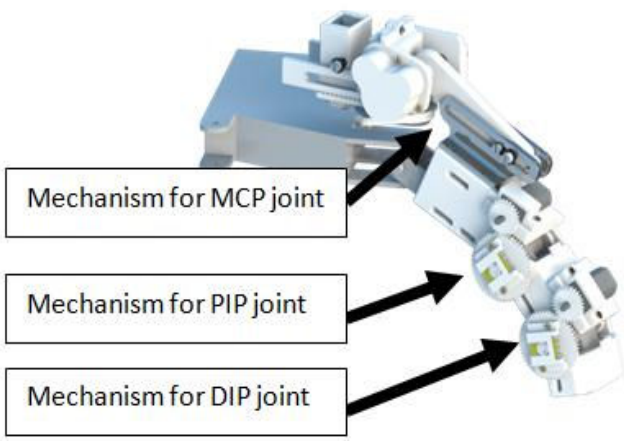

Fig. 2. CAD drawing of the overall mechanical system.

C. Mechanism for the MCP joint module

The MCP joint has two DOFs, abduction/adduction and flexion/extension. The range of motion (ROM) of abduction/adduction for an average adult is up to 45 deg, and the ROM of flexion/extension is about 90 deg [12]. The actuation for the abduction/adduction can be archived by a pair of spur gear sets, in which the axis of the output gear coincides with the axis of abduction/adduction of the MCP joint. However, the same choice is not suitable for the flexion/extension motion. Since the MCP joints of the four fingers are separated from each other with the skin cleft, no external components can be inserted in between. A logical choice is to place the actuation mechanism on the back of the hand and on top of MCP joint. To deliver the force from the actuator to the joint, an articulated mechanism can be used. For safety reasons, only orthogonal force should be applied to the phalanx without having the phalanx pulling away from the joint. Among different articulated mechanisms with one DOF, the Revolute-Prismatic-Revolute-Prismatic (RPRP) configuration meets such requirement. Therefore, it has been implemented in the design. Fig 3 shows the side view of the MCP module.

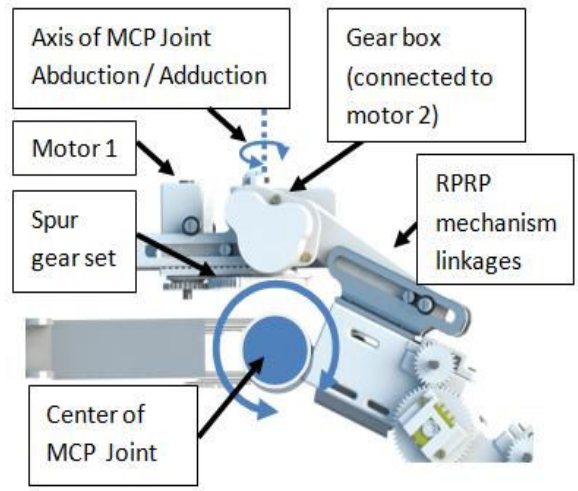

Fig. 3. Side view of the MCP module

As shown in Fig 3, a micro-geared motor (Motor 1) is coupled to a pinion gear to control the abduction/adduction motion. The ratio between the input and output gears is 1:3. Due to safety and space constraints, the ROM is reduced from 60 deg to 25 deg. Another micro-geared motor (Motor 2, not shown in Fig 3) is coupled to an external gear-box that has an input/output ratio of 1:4 to control the motion of flexion/extension. The ROM for such movement is from 0 deg to 90 deg. Two potentiometers are embedded to measure the angular positions of the two joints.

The output of the gear-box actuates the motion of the revolute joint of the RPRP mechanism, and produces an orthogonal force onto the proximal phalanx. Fig. 4 shows the schematic of the MCP module for the flexion/extension motion, a list of parameters which are required to drive the input/output relationship is shown in Table I. Due to the complexity, the equations of the system kinematic and static analysis are not presented in this paper. However the kinematic analysis of the mechanism shows that singularity-free operation can be obtained if the two lengths d_1 and d_2 are made equal (see Fig. 4). It can also be shown that under this circumstance, the stroke of the two prismatic joints D and B also equals d_1 and d_2. Otherwise a singularity occurs when $\theta = 0$ deg.

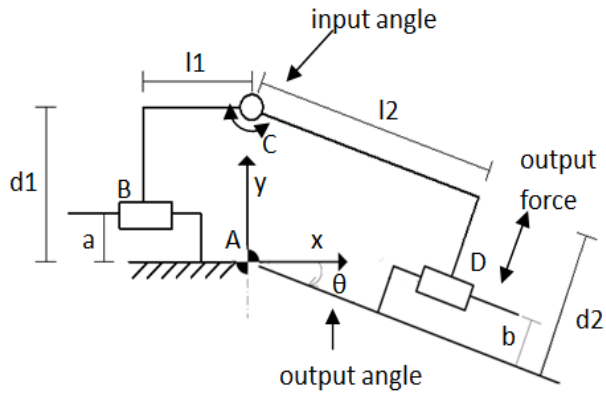

Fig. 4. Schematic of MCP module for flexion/extension

TABLE I
PARAMETERS OF THE RPRP MECHANISM OF THE MCP MODULE

Symbol	Type	Description
A	Revolute joint	MCP joint (output joint)
B	Prismatic joint	Slider between the base and the motor-and-gear compartment
C	Revolute joint	Input of the system
D	Prismatic joint	Slider between the proximal phalanx and the motor-and-gear compartment
a	Distance	Distance between the joint B and the reference frame
b	Distance	Distance between the joint D and the center line of the proximal phalanx
d1	Distance	Height of joint C with respect to the reference base
d2	Distance	Height of joint C with respect to the center line of the proximal phalanx
l1	Distance	Horizontal distance between joint C and B
l2	Distance	Horizontal distance between joint C and D with respect to the center line of the proximal phalanx
θ	Angle	Output angle

D.Mechanism for the PIP and DIP joint module

Compared to the MCP joint module, the mechanism used for the design of PIP and DIP joint is simpler. Due to the fact that both PIP and DIP joints have only 1 DOF, and both have empty gap in between the fingers, external components can be placed on the side of the phalanx. As shown in Fig 5, two micro geared motors are mounted on top of the proximal and medial phalanxes. Each motor is connected to a pinion spur gear which is coupled to the output gear with a ratio of 1:2. The output gear is coaxial with the axis of rotation of the corresponding joint. Two potentiometers are coupled to the output gear to measure the angular joint position for control purpose. Mechanical stoppers are implemented to constrain the ROM of PIP and DIP joints from 0 deg to 90 deg for safety reasons.

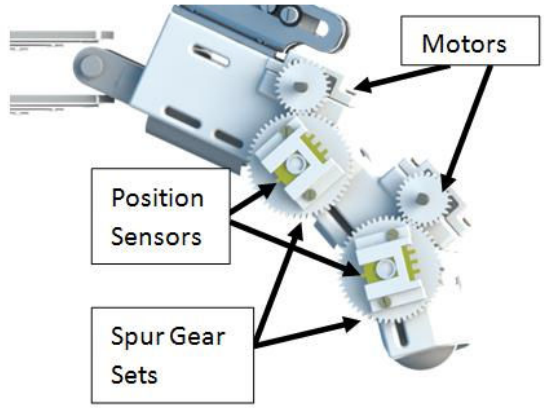

Fig. 5. CAD drawing of the PIP and DIP module

E. Index finger exoskeleton prototype

The design of the exoskeleton has been prototyped using 3D printer. The materials of the prototype mainly consist of ABS plastic. Including the motors, gears and the hand brace, the total weight is around 300 grams. Without the hand brace, the total weight is around 150 grams, which is similar to the one proposed in [11] (120 grams) and lighter than the one in [10] (230 grams). Also, the proposed design in [9]-[11] use cable actuation, large cable boxes are placed external to the hand which made them less portable. Fig 6 shows a volunteer wearing the device. The MCP module of the prototype is mounted on a hand brace which is made of composite material, and the PIP and the DIP modules are secured to the finger with Velcro strap. The characteristic of the prototype is shown in Table II.

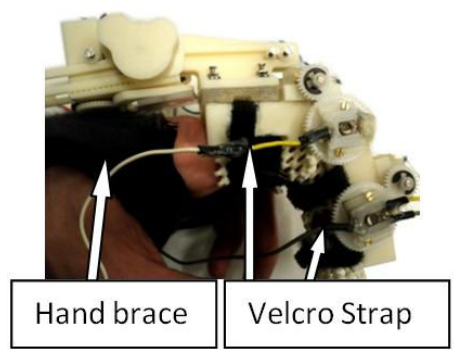

Fig. 6. Index finger exoskeleton prototype

TABLE II
CHARACTERISTIC OF THE EXOSKELETON PROTOTYPE

Actuated DOF	Micro Geared Motor Ratio	Max RPM	Max Torque	Added Gear Ratio
MCP abd/add	298:1	15	0.8 Nm	3:1
MCP flex/ext	298:1	15	1 Nm	4:1
PIP flex/ext	210:1	15	0.6 Nm	2:1
DIP flex/ext	210:1	15	0.6 Nm	2:1

Abbreviation: abd-abduction; add-adduction; flex-flexion; ext-extension.

III. POSITION CONTROLLER DESIGN

The exoskeleton prototype utilizes four high gear ratio motors for actuation, which allows light weight and compact design. However, the effect of friction within the system becomes more significant and it is highly non-linear at low velocity. Simple linear approaches such as a PID controller have been tested and the result showed that it was not sufficient to effectively control the system. In order to construct an effective controller, a system model was created using system identification technique, and an advanced position tracking PID controller with friction compensation was designed and tested. Due to the complexity of the design, only the work on the PIP joint is presented in this paper. However, because of the fact that the DIP joint module has the same configuration as the one of PIP, the same design procedure can be adapted. The system identification approach is described in *sub-section A*, following by the controller design in *sub-section B*, and the performance of system is presented and discussed in *sub-section C*.

A. System Identification for PIP joint module

The model of the PIP joint module is implemented into two distinct parts: the linear part, which describes the overall dynamic of the system; and a second part, which accounts for the term T_{load}, where the frictional model was implemented. The system block diagram of the PIP joint module is shown in Fig. 7, and the list of parameters is shown in Table III.

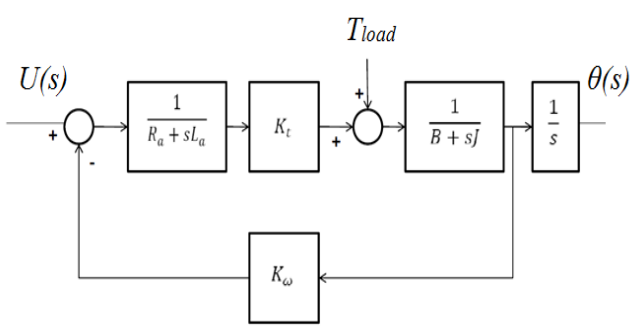

Fig. 7. System block of the PIP joint module

TABLE III
SYSTEM PARAMETERS OF THE PIP JOINT MODULE

Symbol	Description
$U(s)$	Voltage (**input** of the system)
$\theta(s)$	Angular position of the motor shaft (**output** of the system)
T_{load}	External load, includes friction component
R_a	Resistance of the motor
L_a	Inductance of the motor
B	Viscous coefficient of the motor
K_ω	Back-EMG constant
K_t	Torque constant
J	Inertial of the system

Among the parameters list in Table III, R_a, L_a and B are determined by experimental test; and K_ω, K_t and J are estimated using "Grey box" system identification tool from MATLAB. The external load T_{load}, takes into account for the effect of friction on the joint. Such contribution can be accurately described by Stribeck friction model.

According to Stribeck's model [13], friction in a rotary joint can be modelled as a disturbance torque T_{load} defined as:

$$T_{load}(\omega) = T_c + (T_s - T_c)e^{\left|\frac{\omega}{v_s}\right|^{\delta_s}} \qquad (1)$$

being ω the rotational speed of the joint, T_c the Coloumb friction coefficient, T_s the static friction coefficient. v_s is a coefficient known as Stibeck speed, while δ_s is an empirical coefficient. This model accounts for the non-linear characteristic of the friction at low speed. Such contribution should not neglected, since according the evaluated model (estimated parameters are shown in Table IV) friction at low speed can reach values up to 200 mNm. The input of the system identification test is an alternating voltage, *U(s)*, and the output is angular position of the joint, *θ(s)*; the simulation result is shown in Fig.8. With the Stribeck friction model, the system fit is able to reach 87.81%.

TABLE IV
STRIBECK FRICTION COEFFICIENTS FOR THE PIP JOINT

Coefficient	Value	Unit
T_s	0.1991	Nm
T_c	0.0195	Nm
v_s	0.0009	rad/s
δ_s	2.0573	(n/a)

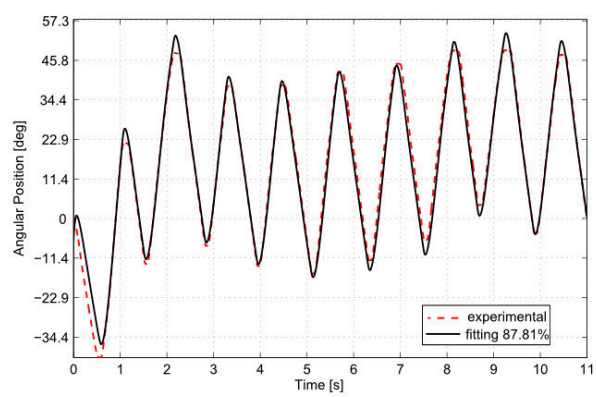

Fig. 8. Simulation of the model's response with Stribeck friction model

B. PID controller with friction compensation

A position control has been implemented by using a PID control system and a feedforward friction compensation (FC) block. A prototype of the Real-Time controller has been implemented using LabView 2009. The block diagram of the controller is shown in Fig.9. The error between the desired and current angular position is sent to the PID controller to generate the first internal output signal. The parameters of the PID controller have been tuned using

genetic algorithm in order to produce best performance. The control action is calculated as the sum of both the outputs of the PID and of the FC block. The value of the friction compensation action is calculated using Eq. (1).

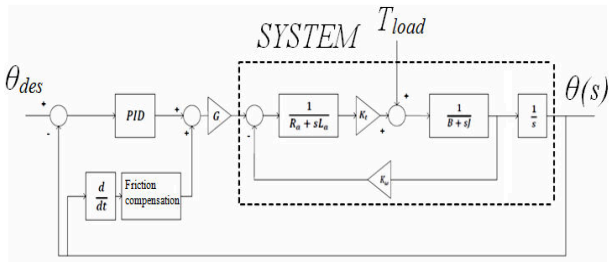

Fig. 9. Block diagram of the PID controller with friction compensation

Moreover the FC block is cascaded with a lead-lag compensator, which experimentally proved to provide a more accurate position tracking. The transfer function of the lead-lag compensator is shown in Eq. 2:

$$Output = G\frac{sT_{lead}+1}{sT_{lag}+1}Input \quad (2)$$

where G is the gain; the T_{lead} is the lead time, and T_{lag} is the lag time, they both express in minutes. The performance of the controller is shown in the following sub-section.

C. System performance

The position tracking controller for the PIP joint module is tested with a sinusoid position reference signal at 0.1Hz and 1Hz. The responses of the closed-loop performance for the two different references are shown in Fig 10 and Fig 11 respectively. Each figure has two sub plots, the subplot (a) shows the system performance without friction compensation, and subplot (b) shows the performance with compensation. The blue dashed lines in the plots are the set point values and the green solid lines are the actual positions of the PIP joint, both measured in degrees [deg]. The x-axes of the plot shows the duration of the test, which is measured in second [sec].

The effects of friction proved to be particularly evident in the first test case (reference signal at 0.1 Hz), because of the low speed of the set point trajectory. As shown in Fig 10 (a), the behaviour of the system is discontinuous and the controller cannot move the device smoothly. At low velocity the system dynamics is nonlinear, and due to the frictional effects there is a dead zone in the duty cycle values within which the actions of the controller are ineffective. As shown in Fig 10 (b), the action of the FC block makes the system response more continuous and smoother. However, there is still discontinuity when the direction switching occurs, which need to be improved in the future.

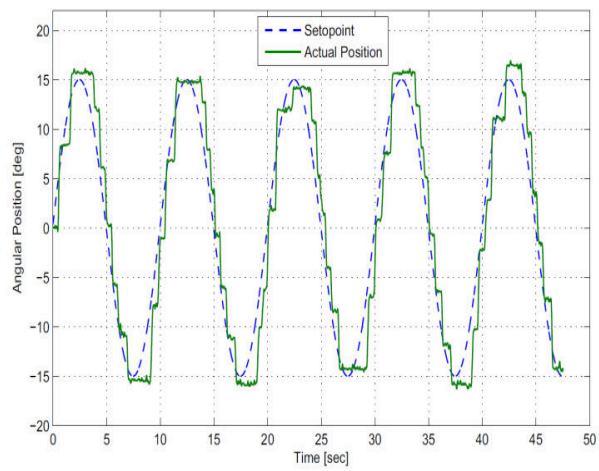

(a) without friction compensation

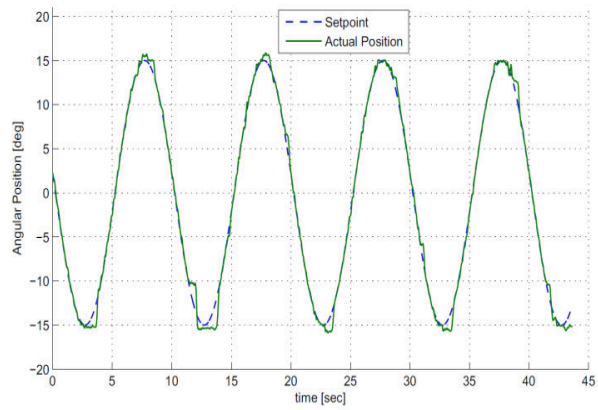

(b) with friction compensation

Fig. 10 - System performance at 0.1 Hz

As the frequency of the sinusoidal reference is increased to 1 Hz, the effect of the friction becomes less evident, and the system is able to behave smoothly even without the FC (see Fig. 11). However, a delay of about 0.1 to 0.2 seconds is noticeable at place where the direction switching of the input occurs. This may be caused by the effect of backlash at the joints. With the FC added, the tracking performance is slightly improved and a smaller delay can be noticed.

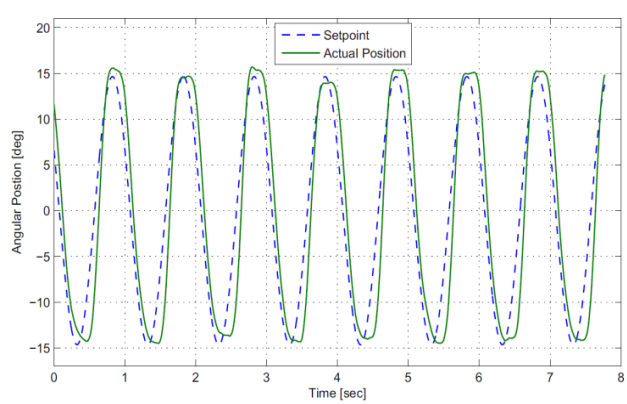

(a) without friction compensation

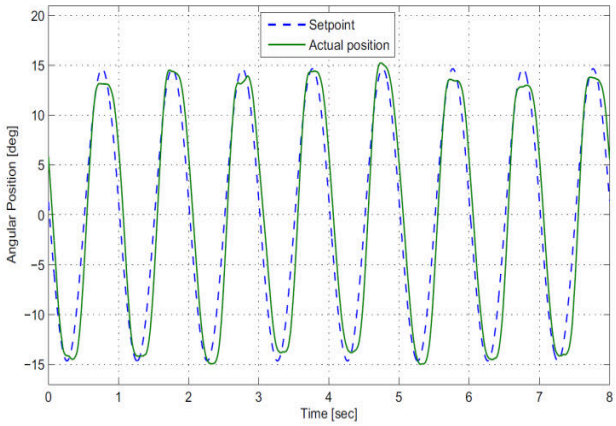

(b) with friction compensation

Fig. 11 - System performance at 1 Hz

A test with a user wearing the exoskeleton was performed to investigate the robustness of the controller. A 0.5 Hz sinusoidal signal is fed into the system as input for position tracking. The system rotates the proximal phalanx at the input frequency while the user does not provide any active resistant force. In this way only the passive impedance of the index is acting as a disturbance on the device. The result of the test is shown in Fig 12. The recorded system response shows that the system is capable to track the angular position accurately with a small and consistent delay. A reduction of the amount of delay and the investigation of the effect of resistive load from the user will be performed in future works.

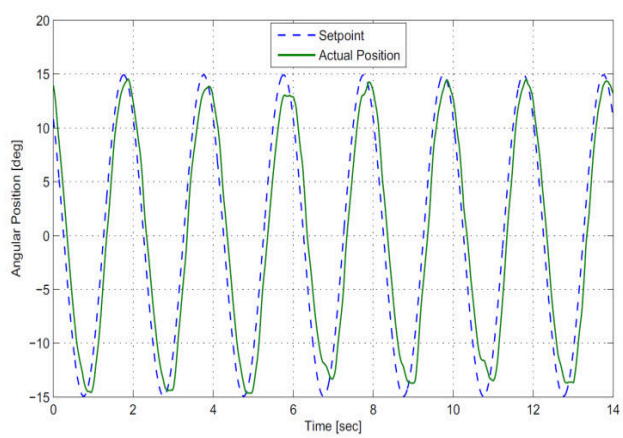

Fig. 12 - Performance test with user wearing the device

IV. Conclusion

In this paper a novel exoskeleton for the post-stroke rehabilitation of the index finger has been presented. The device has a compact and low weight design, and it can be worn without interfering with the grasp of the patient. It has four active DOFs for controlling the movement of each the finger joint, therefore allowing the user to perform complex functional rehabilitation routines. A working prototype has been built and tested. A model-based position control with friction compensation has been developed, and the effectiveness of the proposed approach has been shown trough experimental tests. A small delay is noticed in the tests, which should be improved in future works. Also, the effect of active load from the user should be investigated.

Acknowledgment

The authors would like to acknowledge Ausama Ahmed for his assistance with electrical components selection and suggestion on the controller and software design.

References

[1] "Statistics", Heart & Stroke Foundation. Available: http://www.heartandstroke.com/site/c.ikIQLcMWJtE/b.3483991/k.34A8/Statistics.htm#stroke

[2] R. A. R. C. Gopura and K. Kiguchi, "Mechanical designs of active upper-limb exoskeleton robots: State-of-the-art and design difficulties," in *2009 IEEE International Conference on Rehabilitation Robotics*, 2009, pp. 178-187.

[3] N. Benjuya, S. B. Kenney, *Myoelectric Hand Orthosis*, Journal of rosthetics and Orthosis, 1990, Vol. 2, Num. 2, pp 149–154

[4] M. Bouzit, G. Popescu, G. Burdea, R. Boian, *The Rutgers Master II-ND Force Feedback Glove*, Proceedings of the 10th Symposium On Haptic Interfaces For Virtual Environment and Teleoperator Systems, HAPTICS '02.

[5] R.C.V. Loureiro, W.S. Harwin, Reach & Grasp Therapy: Design and Control of a 9-DOF Robotic Neurorehabilitation System, Proceedings of the 2007 IEEE 10th International Conference on Rehabilitation Robotics, June 12-15, Noordwijk, The Netherlands.

[6] E.J. Koeneman, R.S. Schultz, S.L. Wolf, D.E. Herring, J.B. Koeneman, A Pneumatic Muscle Hand Therapy Device, Engineering in Medicine and Biology Society, 2004. IEMBS'04. 26th Annual International Conference of the IEEE, Vol 1 pp 2711-2713

[7] L. Dovat, O. Lambercy, R. Gassert, T. Maeder, T. Milner, T. Chee Leong, E. Burdet, *HandCARE: A Cable-Actuated Rehabilitation System to Train Hand Function After Stroke*, IEEE Transactions on Neural Systems and Rehabilitatio Engineering, Vol. 16, No. 6, December 2008.

[8] S. Ueki, Y. Nishimoto, M. Abe, H. Kawasaki, S. Ito, Y. Ishigure, J. Mizumoto, T. Ojika, *Development of Virtual Reality Exercise of Hand Motion Assist Robot for Rehabilitation Therapy by Patient Self-Motion Control*, 30th Annual International IEEE EMBS Conference Vancouver, British Columbia, Canada, August 20-24, 2008.

[9] A. Wege, G. Hommel, Development and Control of a Hand Exoskeleton for Rehabilitation of Hand Injuries, Intelligent Robots and Systems, 2005.(IROS 2005). 2005 IEEE/RSJ International Conference on, pp 3046-3051

[10] T.T. Worsnopp, M.A. Peshkin, J.E. Colgate, and D.G. Kamper, An Actuated Finger Exoskeleton for Hand Rehabilitation Following Stroke, Proceedings of the 2007 IEEE 10th International Conference on Rehabilitation Robotics, June 12-15

[11] J. Wang, J. Li, Y. Zhang, S. Wang, *Design of an Exoskeleton for Index Finger Rehabilitation*, Engineering in Medicine and Biology Society, 2009. EMBC 2009. Annual International Conference of the IEEE, pp 5957-5960

[12] M. Nordin, V.H. Frenkel, Basic Biomechanics of the Muscoloskeletal System (3rd ed.), 2001, Lippincott Williams & Wilkins.

[13] L. Marton, and B. Lantos, *Control of mechanical systems with Stribeck friction and backlash*, System and Control Letters, 58 (2), pp. 141-147, 2009